



Deposited via The University of Sheffield.

White Rose Research Online URL for this paper:

<https://eprints.whiterose.ac.uk/id/eprint/219739/>

Version: Accepted Version

---

**Proceedings Paper:**

Alblooshi, A. and Masoud, M.I. (2022) Design of a 1 MW grid-tied photovoltaic system. In: 2021 International Conference on Engineering and Emerging Technologies (ICEET). 2021 International Conference on Engineering and Emerging Technologies (ICEET), 27-28 Oct 2021, Istanbul, Turkey. Institute of Electrical and Electronics Engineers (IEEE). ISSN: 2409-2983. EISSN: 2409-2983.

<https://doi.org/10.1109/iceet53442.2021.9659704>

---

© 2021 IEEE. Personal use of this material is permitted. Permission from IEEE must be obtained for all other users, including reprinting/ republishing this material for advertising or promotional purposes, creating new collective works for resale or redistribution to servers or lists, or reuse of any copyrighted components of this work in other works. Reproduced in accordance with the publisher's self-archiving policy.

**Reuse**

Items deposited in White Rose Research Online are protected by copyright, with all rights reserved unless indicated otherwise. They may be downloaded and/or printed for private study, or other acts as permitted by national copyright laws. The publisher or other rights holders may allow further reproduction and re-use of the full text version. This is indicated by the licence information on the White Rose Research Online record for the item.

**Takedown**

If you consider content in White Rose Research Online to be in breach of UK law, please notify us by emailing [eprints@whiterose.ac.uk](mailto:eprints@whiterose.ac.uk) including the URL of the record and the reason for the withdrawal request.

# Design of a 1 MW Grid-tied Photovoltaic System

Abdelrahman Alblooshi  
Electronic and Electrical Engineering Department  
Faculty of Engineering, University of Sheffield  
Sheffield, the UK  
abdelrahman981s@gmail.com

Mahmoud I. Masoud  
Electronic and Electrical Engineering Department  
Faculty of Engineering, University of Sheffield  
Sheffield, the UK  
m.masoud@sheffield.ac.uk

**Abstract**—The installation of large-scale grid-tied photovoltaic (PV) systems are rising fast around worldwide. This rise is because the system relies on a widely available green source (sun). Furthermore, many developments were carried out to increase the PV system efficiency and decrease its total cost, which encouraged electrical companies to install large-scale PV systems. Many components must be used to construct an efficient system, including a PV array, two power electronics converters, filter and transformer. Additionally, two controllers are usually in the design. One is in charge of maximising the power for the PV modules in the array, and the second one is used to ensure the voltage is constant. The paper introduces a PV system design that can reach 1 MW connected to the grid through different stages to match up with the required voltage and frequency of the grid as a requirement for the final year project in electronic and electrical engineering department, University of Sheffield. The whole grid-tied PV system was designed and simulated using MATLAB/SIMULINK.

**Keywords**—Boost converter, dq-controller, Grid-tied Photovoltaic system, LCL filter, Maximum power point tracker (MPPT), Three-phase inverter

## I. INTRODUCTION

Generating energy using renewable energy resources can tackle future energy demand, which is expected to happen due to the limited availability of fossil fuels. One of the best alternatives considered is large-scale grid-tied photovoltaic (PV). Nowadays, researchers increase the PV system efficiency and decrease its total cost, encouraging electrical companies to install large-scale PV systems. Moreover, it mitigates the excessive usage of fossil fuels. There are already many PV power plants that were installed around the world. According to the latest renewable capacity statistics made by an international energy agency, the global generating capacity of PV systems jumped by 115 GW in 2019 to reach 627 GW. The overall contribution of the PV system in generating energy demand was approximately 3% of the worldwide energy demand [1]. Additionally, 59% of the energy generated from renewable sources was from the PV system, mainly because of how cost-efficient the PV systems have become [1]. In 2020, Sheffield solar estimated a 13 GW of total cumulative capacity of a PV system installed in the UK, which supplies about 13% of the total energy demand in the UK. The all-time peak power generation from the installation reached about 9.68 GW in April 2020 [2]. Those numbers show how well trusted grid-tied PV systems are seen as a future solution for worldwide energy security.

There are two topologies for the grid-tied PV system; single-stage and two-stages. The difference between the two configurations is that the two-stage system has one more component added to it, called DC/DC converter; thus, the two stages are more expensive and more complicated to design

than the single-stage. For the single-stage system, the inverter is directly connected to the PV system. Where two objectives are carried across the inverter by the same controller, the first objective maximises the power extracted from the PV using the maximum power point tracker (MPPT). The second objective of the controller is to generate the pulse width modulation (PWM) for the inverter to regulate the voltage [3]. However, this imposes some difficulty in getting the required DC voltage, which leads to some restrictions in extracting the maximum power. To overcome this issue, a DC/DC converter can be added before the inverter; therefore, two controllers are required, one for the DC/DC converter to carry the MPPT and the second is for the inverter to regulate the voltage; this will enhance the MPPT operation [3]. The focus of this paper will be on the two-stages topologies, whereas the single-stage system will be mentioned solely for some comparison between the PV array construction of the two systems.

This paper aims to show how to construct a full grid-tied PV system in MATLAB/SIMULINK and show how each component of the system contributes to obtaining the required parameters for the system. Moreover, the paper will also include some comparisons between the single-stage and two-stages PV system configurations. Hence, the target is to design the entire system of a 1MW grid-tied PV system, as shown in fig 1. to fulfil the requirement of the final year project. The project was individual, and last year we had a difficult time due to COVID-19, where we had a continuous lockdown which was one of the obstacles to cover all the project requirements. Nonetheless, the student did excellent work and accepted the challenge.

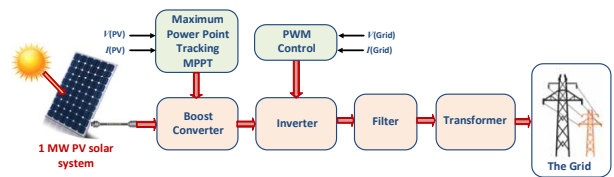


Fig. 1. Block diagram of grid-tied PV system

After this introduction, the system description is introduced in section II. Section III presents the design to achieve the required specifications. This section includes the data for the selected components. Section IV presents the design evaluation using MATLAB/SIMULINK and a detailed discussion of the system outcomes. The conclusion is given in section V.

## II. SYSTEM DESCRIPTION

Several components must be installed and connected to produce significant power to construct a large-scale grid-tied PV system, as shown in Fig. 1. Those components include PV array, DC/DC converter, inverter, filter, and transformer. The PV array is built using several PV modules, and it is the

system's power source [4]. The PV array behaviour depends mainly on two things: solar irradiance and temperature. The PV array produces a smaller current and lower power when solar irradiance is reduced [5]. Changing the temperature would mainly change the PV array output voltage, and the higher the temperature, the lower the power [5].

The PV array must be operating at the maximum power point at all times; this can happen using MPPT controllers. There are several types of MPPT; one of the most suitable algorithms of MPPT is Perturb and observe (P&O), which has good tracking behaviour, and it is less complex to design in comparison to other topologies [6]-[8].

The second component is the DC/DC converter. Several types can be used in the PV system. Eleven of them were mentioned in literature [9]. Each has its benefits and drawbacks compared to the others. The most common converters are boost, buck, buck-boost converters. The buck steps down the DC voltage to a lower value; hence it is suitable for low battery application. Secondly, the boost converter can step up the DC voltage to higher voltage; thus, useful for high load application. Lastly, the buck-boost can either step up or step down the voltage depending on the polarity setting. Literature [9] mentioned that buck-boost is the most efficient converter between the three; however, it only operates efficiently with low load and is not helpful for large systems. Therefore the best choice for the proposed system would be the boost converter due to its stepping up ability. Between the boost and the inverter, there is a capacitor bank which is also called DC-link. It is used to minimise the DC voltage fluctuation before passing it to the inverter [10].

The voltage coming from the boost can then be converted from DC to AC using an inverter to match up with the AC grid. The inverter in the PV system can be controlled using a closed-loop dq controller. This dq controller has two cascaded loops, the inner and the outer loop. The inner loop regulates the current at the grid; therefore, it is responsible for power quality and current protection. On the other hand, the outer loop manages the DC voltage at the capacitor bank; thus, it is responsible for the power flow [11]. This controller transfers the three-phase grid voltage and current into a DC value to simplify the controlling and filtering. Moreover, the DC voltage of the boost converter is compared to the reference value set inside of this controller, which helps maintain a constant voltage in the system [11].

The AC voltage produced by the inverter usually contains large harmonics; hence, a filter needs to get rid of them. According to reference [12], three simple filter topologies can be used: L-filter, LC-filter, and LCL-filter. The best of the three is the LCL filter because it has a low switching frequency and does not rely on the grid impedance due to its decoupling ability [12]. After minimising the harmonics to a tolerated amount, the voltage is stepped up using a transformer that matches the system voltage with the large grid voltage.

### III. SYSTEM DESIGN

The design of the full grid-tied PV system requires that each component be designed and tested individually, then connect the components to form the whole system. This helps to check if the parts are behaving as expected or whether it requires more adjustment. The design requirements and constraints are listed in Table I.

TABLE I: Design requirements

Parameters	values
PV Array configuration (parallel × series)	Parallel modules: 159 ( $V_{pv}=750$ V) Series modules: 20 ( $I_{pv}=1333$ A)
PV Array power at (25 °C and 1000 W/m <sup>2</sup> )	1 MW
Boost converter voltage	1500 V
Filter voltage (phase to phase)	730 V
Transformer Turn ratio	n1:n2 = 730 V: 11 kV
Grid voltage	11 kV

The first part of the design was to build the PV array by calculating the total number of series connections of the PV modules ( $N_s$ ) and the total parallel string ( $N_p$ ) using (1) and (2).

$$N_s = \frac{V_{pv}}{V_{mp}} \quad (1)$$

$$N_p = \frac{\left(\frac{P_{max}}{V_{pv}}\right)}{I_{mp}} \quad (2)$$

$P_{max}$  is the maximum power obtained under nominal temperature (25°C) and nominal solar irradiance (1 kW/m<sup>2</sup>). The targeted power is 1 MW.  $V_{pv}$  is the targeted PV array voltage (750 V),  $I_{mp}$  and  $V_{mp}$  are the maximum current and voltage of the selected PV module (TSM-315pa14a) [13]. The parameters of the selected PV module is illustrated in the Appendix. Based on (1) and (2) and design requirements, the number of modules in series are 20, and the number of modules in parallel is 159.

The boost converter components and the DC-link capacitor are calculated using (3) to (5) [14][15].

$$L_{boost} = \frac{V_{pv} \times (V_{boost} - V_{pv})}{f_s \times \Delta I_L \times V_{boost}} \quad (3)$$

$$C_{in} = \frac{D}{R_{load} \times f_s \times \left(\frac{\Delta V}{V_o}\right)} \quad (4)$$

$$C_{link} = \left(\frac{2 \times P_{max}}{V_{min}^2 \times f_{grid}}\right) \quad (5)$$

The boost converter is shown in fig. 2. The value  $L_{boost}$  is the boost converter inductor,  $C_{in}$  is a capacitor between the PV array and boost converter, and  $C_{link}$  is the DC-link capacitor between the boost converter and the inverter., Note for a large PV system, there is a need for a large DC-link capacitor ( $C_{link}$ ), and it is formed from a group of series and parallel capacitors to achieve the required value. The designed capacitor is 0.04 F and 1500 V. This rating achieves settling time 0.63s, ripple voltage 7.3 V, and ripple current 1.2 A. To accomplish this, select 68 capacitors from ALS70A1: (10000 μF, 500 VDC) [16], where the string consists of four capacitors connected in series to add safety margins and 17 capacitors connected in parallel. The total capacitance will be 43 mF which satisfies the requirements.

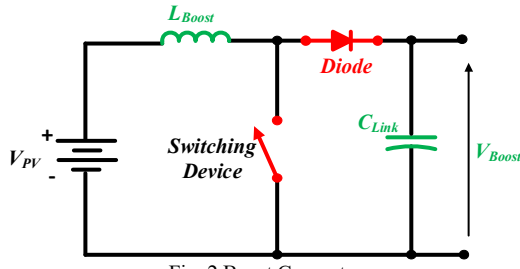


Fig. 2 Boost Converter

The switching scheme of the boost was manipulated using a duty cycle generated by the perturb and observe (P&O) MPPT controller. Fig. 3 shows the flowchart of the controller. Table II illustrated the designed values for the boost converter.

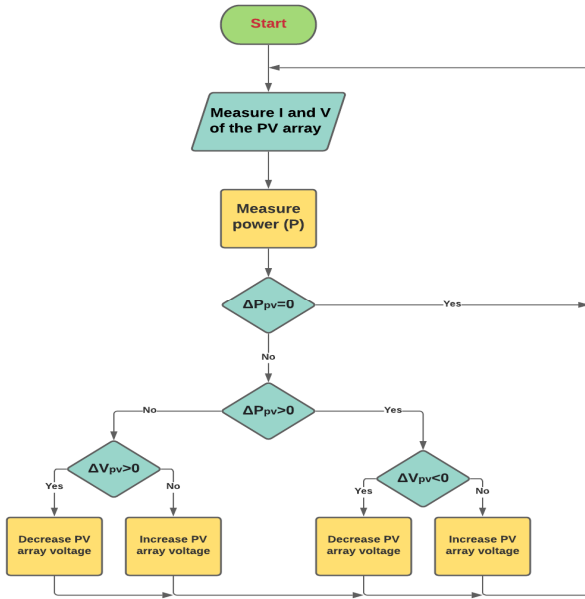


Fig. 3. Flowchart of P&O MPPT

TABLE II: Boost Converter Design values

Component	value
$C_m$ (capacitor connected to PV module)	8.9 mF
Boost inductor	70.3 mH
$C_{link}$ (capacitor links boost and inverter)	42.5 mF
Switching frequency	2 kHz
Duty cycle	0.5 s

The next stage is to design the three-phase inverter to convert the DC voltage at the DC-link to AC. The inverter was controlled using a dq controller illustrated in Fig. 4. Two PI controllers are used. The values for proportional gain  $K_p$  and integral gain  $K_i$  used in the PI were found using trial and error. Furthermore, a phase-locked loop (PLL) was implemented to ensure the controlled current is in phase with the grid voltage. The reference for the reactive power was set to zero, assuming that the system has a unity power factor. At the same time, the DC voltage reference is assigned to the required value 1500 V.

Next, the LCL filter ensures that the AC voltage produced is free from the high harmonics. Equations (6)-(9) were used to obtain the values of the filter parameters [17]. The filter arrangement is shown in fig. 5.

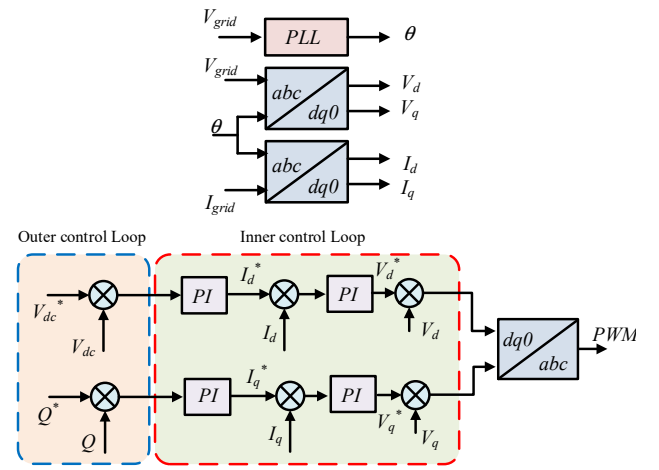


Fig. 4. dq-controller for the inverter

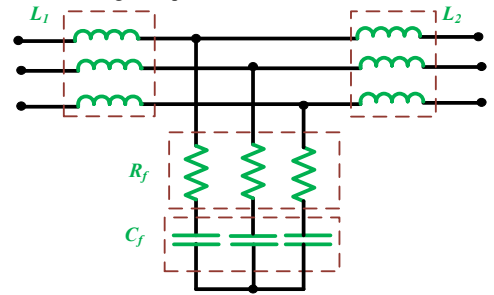


Fig. 5. LCL filter connected to the inverter terminals

$$C_f = 0.05 \times \frac{1}{\frac{V_f^2}{P_{max}} \times 2\pi f_{grid}} \quad (6)$$

$$L_1 = \frac{V_{dc}}{6 \times F_s \times \Delta I_{max}} \quad (7)$$

$L_1$  is the inductor to the inverter side, and  $\Delta I_{max}$  is the accepted ripple current.

$$L_2 = \frac{\sqrt{\frac{1}{k_a} + 1}}{C_f \times 2\pi f_s^2} \quad (8)$$

$L_2$  is the inductor connected to the transformer side. The value  $k_a$  represents the attenuation factor, and  $f_s$  is the switching frequency.

$$R_f = \frac{1}{3 \times C_f \times \omega_{resonance}} \quad (9)$$

$R_f$  is in charge of eliminating underside resonance.

Table III illustrates the values of the designed filter

TABLE III: Boost Converter Design values

Component	value
$L_1$ (inductor to the inverter side)	$2.42 \times 10^{-4}$ H
$L_2$ (inductor to the transformer side)	$1.45 \times 10^{-4}$ H
$C_f$ (Filter capacitor)	$3 \times 10^{-4}$ F
$R_f$ (filter resistor)	0.39 $\Omega$
$F_{resonant}$	972 Hz

Once the high harmonics are eliminated, the PV system is connected to the transformer, which matches the voltage with the 11 kV grid voltage. The grid is simulated as an infinite bus bar. The full PV system is implemented using

MATLAB/SIMULINK. If the boost converter is removed, the system is considered a single-stage PV system.

#### IV. DESIGN EVALUATION AND DISCUSSION

The PV array has 3180 modules arranged in series and parallel. To evaluate the designed PV, check the design requirement given in table I. At the nominal condition of 1 kW/m<sup>2</sup> and 25 °C. Fig. 6a demonstrated how the PV array reacted to that condition and generated a maximum power equal to 1 MW. Accordingly, the maximum capacity 1 MW was then maintained at this point with the aid of the MPPT controller, as shown in Fig. 6b.

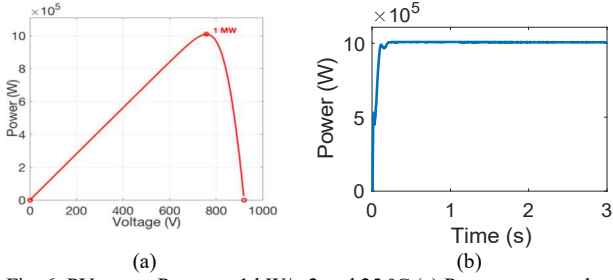


Fig. 6. PV power Power at 1 kW/m<sup>2</sup> and 25 °C (a) Power versus voltage for the PV array, and (b) PV array output power with MPPT

Check different conditions of the solar irradiance and temperature and how the system would be affected. Fig. 7 parts (a) to (d) shows the effect of varied solar irradiance and constant temperature condition. The solar irradiance applied to the PV array varies between 1 kW/m<sup>2</sup>, 0.8 kW/m<sup>2</sup>, and 0.5 kW/m<sup>2</sup> as shown in part (a). Part (b) shows the power output from the PV corresponding to different irradiance values, while part (c) indicates the voltage of the PV array and boost converter. The voltage across the boost converter is maintained at 1500 V. The overshoot is due to the PI controller response. Fig. 7d shows the current. It is clear that at 1 kW/m<sup>2</sup>, the current is 1333 A, while at 0.5 kW/m<sup>2</sup>, the current drops to 670 A.

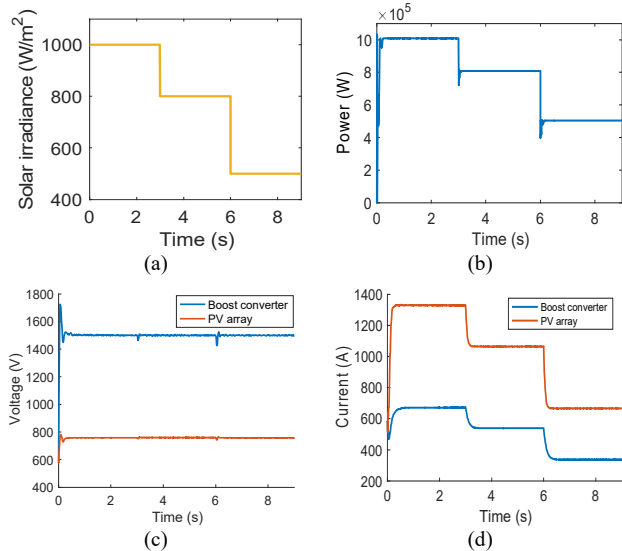


Fig. 7. Effect of solar irradiance at constant temperature (a) Solar irradiance variations (b) PV output power, (c) PV voltage and boost converter voltage, (d) PV current and boost converter current.

The varied temperature and constant solar irradiance condition are shown in Fig. 8. Part (a) shows the stepped temperature variation (0°C, 15°C, and 25°C). Part b

illustrates the PV power, which records the highest value of 1.09 MW when the temperature is set to 0°C. The DC voltage had a different behaviour for PV array and boost converter, where the PV array voltage varied and decreased as the temperature increases. In contrast, the boost converter maintained the steady-state value of 1500 V at all times despite the temperature variation, as illustrated in part (c). Part d shows that the PV current is constant at 1333 A with minor overshoot behaviour at each step. On the other hand, the current passing through the boost converter decreased as the temperature increased mainly to keep the boost voltage constant.

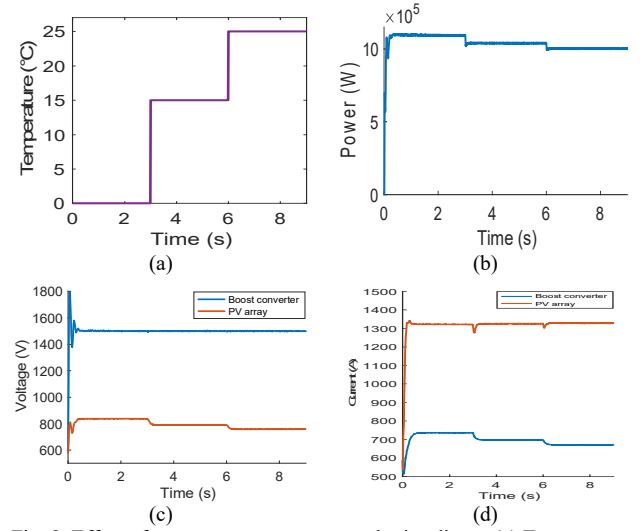


Fig. 8. Effect of temperature at constant solar irradiance (a) Temperature variations (b) PV output power, (c) PV voltage and boost converter voltage, (d) PV current and boost converter current.

The relationship between the varied conditions with current and voltage are normally represented by (10), where  $I_{ph}$  is the photocurrent made by the solar irradiance. The equation clearly demonstrates that the more  $I_{ph}$ , the more the current. Furthermore, the equation also shows that the more the temperature applied to the PV module, the less the voltage produced by the PV module [18].

$$I = C_p I_{ph} - C_p I_0 \left[ \exp \left( \frac{q(V + R_S I)}{C_S A K T} \right) - 1 \right] \quad (10)$$

Fig. 9 shows the inverter stage as the input is 1500 V (DC-value). Part a indicates the inverted voltage waveform full of high-frequency components, as shown in part (b). Subsequently, the LCL filter eliminates those harmonics and creates a clear sinusoidal waveform with a line to line AC voltage equal to 730 V as shown in part c; thus, the filter obtained the specified value. Moreover, the FFT analysis of the filter voltage shown in part d demonstrates that the THD reduced to approximately 2%, satisfying the IEEE standard 519 [20]. Fig. 10 illustrates how the transformer matches the grid voltage, which equals 11 kV.

To have a single-stage system, remove the boost converter. In this case, the PV module arrangement should be modified to have 1500 V. A 3200 modules are required. Forty modules are connected in series per string, and 80 strings are connected in parallel to satisfy the design requirements. This results in an increase of series PV modules in each string, which imposed an issue in comparison to the two-stages

system. A failure in one module will stop the operation of an entire string. In the case of single-stage, it had more series modules, therefore higher risk of losing the operation and becoming unstable. Fig. 11 shows the PV array voltage and current at nominal conditions of  $1 \text{ kW/m}^2$  and  $25^\circ \text{C}$ . The rest of the system has the same results as the two-stage system.

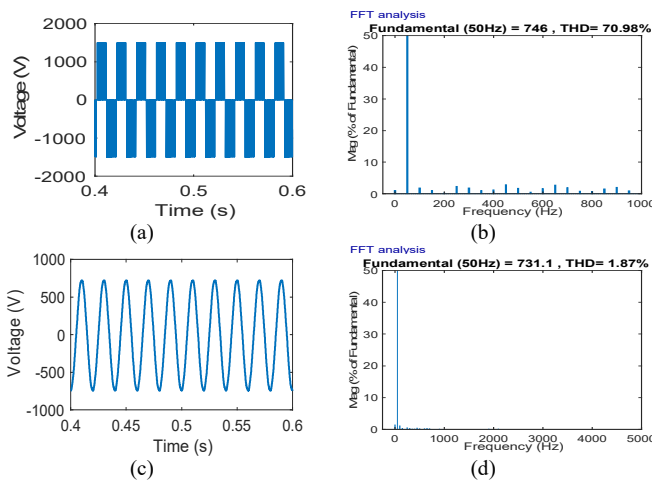


Fig. 9 DC to AC converter (a) Inverter output voltage (b) FFT analysis for inverter output voltage, (c) LCL output voltage, (d) FFT analysis for filter output voltage.

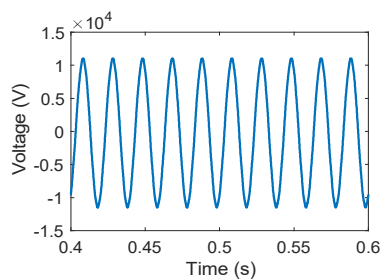


Fig. 10 Transformer voltage

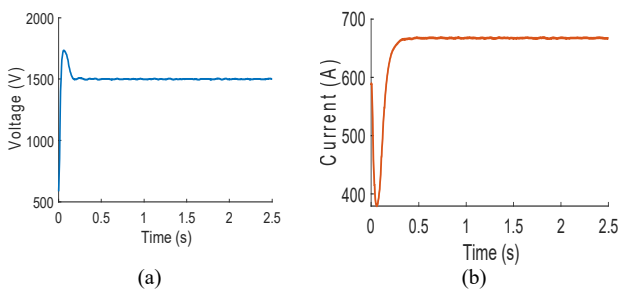


Fig. 11 Single-stage PV system: (a) Voltage across PV array, (b) Current through PV array

The complete grid-tied PV system shown in fig. 1 is designed and tested. The design requirements are achieved. Despite meeting all the required parameters, the system could have used one extra component like a battery or other storage system charged within the PV system. This storage system aims to provide power even if there is no solar irradiance applied to the PV array. Due to the limited space, the cost analysis is out of the scope of this paper.

## V. CONCLUSION

The Electronic and Electrical engineering Department; the University of Sheffield proposes a third-year undergraduate project to design the entire system of a 1MW grid-tied PV system. The project includes the following tasks distributed between two semesters, design of the PV array capable of

delivering the required power (1 MW), design of dc-dc converter with MPPT, and controlled three-phase inverter stage connected to passive filter and transformer then connected to the grid. The whole grid-tied PV system was designed and simulated using MATLAB/SIMULINK. The methodology used to accomplish the project is to design each component and test it individually. Hence, the whole system is combined and tested. The first component was the PV array which produces a voltage approximately equal to 0.75 kV and current equal to 1.33 kA at nominal conditions, achieving a 1 MW power output from the PV. The effect of irradiance and temperature is also investigated. The boost converter is used to step up the voltage to 1.5 kV. The MPPT controller maintains the maximum power for each condition. Subsequently, the three-phase inverter operated as needed by converting the voltage and current at DC-link into AC. The dq controller is used to keep the DC voltage applied to the inverter constant despite the varied conditions of solar irradiance and temperature; hence, a constant voltage is injected into the grid. The LCL filter was able to eliminate the high harmonics and keep the THD value within the required standard. The last stage is the step-up transformer to have voltage 11 kV, which matches the grid. The required functionality of each component was obtained just as needed. A single-stage system was implemented to be compared with the two-stage system. It was shown that more PV modules are required for the single-stage system. Therefore, there is a trade-off between stability and overall system cost.

## REFERENCES

- [1] A. Detollenaere, J. Wetter, G. Masson, I. Kaizuka, A. Jäger-Waldau, and J. Donoso, "Snapshot of Global PV Markets 2020 PVPS Task 1 Strategic PV Analysis and Outreach," 2020, doi: 10.13140/RG.2.2.24096.74248.
- [2] "PV Live – Sheffield Solar." Accessed: Apr. 13, 2021. [Online]. Available: <https://www.solar.sheffield.ac.uk/pvlive/>.
- [3] G.-S. Kim, K.-B. Lee, D.-C. Lee, and J.-M. Kim, "Fault Diagnosis and Fault-Tolerant Control of DC-link Voltage Sensor for Two-stage Three-Phase Grid-Connected PV Inverters," *J. Electr. Eng. Technol.*, vol. 8, no. 4, pp. 752–759, Jul. 2013, doi: 10.5370/JEET.2013.8.4.752.
- [4] V. M. Fthenakis and H. C. Kim, "Photovoltaics: Life-cycle analyses," *Sol. Energy*, vol. 85, no. 8, pp. 1609–1628, Aug. 2011, doi: 10.1016/j.solener.2009.10.002.
- [5] H. Bellia, R. Youcef, and M. Fatima, "A detailed modeling of photovoltaic module using MATLAB," *NRIAG J. Astron. Geophys.*, vol. 3, no. 1, pp. 53–61, Jun. 2014, doi: 10.1016/j.nriag.2014.04.001.
- [6] H. N. Zainudin and S. Mekhilef, "Comparison Study of Maximum Power Point Tracker Techniques for PV Systems," p. 6.
- [7] P. Mohanty, G. Bhuvanewari, R. Balasubramanian, and N. K. Dhaliwal, "MATLAB based modeling to study the performance of different MPPT techniques used for solar PV system under various operating conditions," *Renew. Sustain. Energy Rev.*, vol. 38, pp. 581–593, Oct. 2014, doi: 10.1016/j.rser.2014.06.001.
- [8] T. Eram and P. L. Chapman, "Comparison of Photovoltaic Array Maximum Power Point Tracking Techniques," *IEEE Trans. Energy Convers.*, vol. 22, no. 2, pp. 439–449, Jun. 2007, doi: 10.1109/TEC.2006.874230.
- [9] K. V. G. Raghavendra, K. Zeb, M. Anand, P. Kumar, D. Kim, M. Kim et al., "A Comprehensive Review of DC–DC Converter Topologies and Modulation Strategies with Recent Advances in Solar Photovoltaic Systems," *Electronics*, vol. 9, no. 1, p. 31, Dec. 2019, doi: 10.3390/electronics9010031.
- [10] Jalmodovar, "DC-Link Design Tips," *Engineering Center*, Oct. 01, 2019. <https://ec.kemet.com/blog/dc-link-design-tips/> (accessed Apr. 13, 2021).
- [11] F. Blaabjerg, R. Teodorescu, M. Liserre, and A. V. Timbus, "Overview of Control and Grid Synchronization for Distributed Power Generation

- Systems,” *IEEE Trans. Ind. Electron.*, vol. 53, no. 5, pp. 1398–1409, Oct. 2006, doi: 10.1109/TIE.2006.881997.
- [12] K. A. El Wahid Hamza, H. Linda, and L. Cherif, “LCL filter design with passive damping for photovoltaic grid connected systems,” in *IREC2015 The Sixth International Renewable Energy Congress*, Sousse, Tunisia, Mar. 2015, pp. 1–4, doi: 10.1109/IREC.2015.7110945.
- [13] “SolarHub - PV Module Details: TSM-315PA14A.08 - by Trina Solar.” Accessed Apr. 21, 2020. [Online]. Available:<http://www.solarhub.com/product-catalog/pv-modules/34586-TSM-315PA14A-08-Trina-Solar>
- [14] “Environmental Impacts of Solar Power | Union of Concerned Scientists.” Accessed: Apr. 25, 2021. [Online]. Available: <https://www.ucsusa.org/resources/environmental-impacts-solar-power>
- [15] M. D. Vijay, I. Hussain, B. Singh, and G. Bhuvaneswari, “Energy management and control of SECS and BESS integrated AC microgrid,” in *2017 IEEE 26th International Symposium on Industrial Electronics (ISIE)*, Edinburgh, United Kingdom, Jun. 2017, pp. 975–980, doi: 10.1109/ISIE.2017.8001378.
- [16] “ALS70A103NT500 KEMET | Mouser,” *Mouser Electronics*. Accessed May. 06, 2021. [online]. Available: <https://eu.mouser.com/ProductDetail/80-ALS70A103NT500>
- [17] H. Yatimi and E. Aroudam, “Mathematical Modeling and Simulation of Photovoltaic Power Source using Matlab/Simulink,” vol. 16, no. 2, p. 9, 2016.
- [18] “IEEE Recommended Practices and Requirements for Harmonic Control in Electrical Power Systems,” *IEEE Std 519-1992*, pp. 1–112, Apr. 1993, doi: 10.1109/IEEESTD.1993.114370.

## Appendix

Parameters of TSM-315PA14A.08 [13]

Parameters	values
Cells per module	72
Open circuit voltage ( $V_{oc}$ )	46 V
Short-circuit current ( $I_{sc}$ )	8.86 A
Current at maximum power point ( $I_{mp}$ )	8.38 A
Maximum power	315 W
The voltage at maximum power point ( $V_{mp}$ )	37.9 V
Area	1.92 m <sup>2</sup>
$K_i$ (temperature coefficient)	0.05